

Visual-Tactile Sensory Map Calibration of a Biomimetic Whiskered Robot

Tareq Assaf¹, Emma D.Wilson²,
Sean Anderson², Paul Dean², John Porrill² and Martin J.Pearson¹

Abstract—We present an adaptive filter model of cerebellar function applied to the calibration of a tactile sensory map to improve the accuracy of directed movements of a robotic manipulator. This is demonstrated using a platform called *BellaBot* that incorporates an array of biomimetic tactile whiskers, actuated using electro-active polymer artificial muscles, a camera to provide visual error feedback, and a standard industrial robotic manipulator. The algorithm learns to accommodate imperfections in the sensory map that may be as a result of poor manufacturing tolerances or damage to the sensory array. Such an ability is an important pre-requisite for robust tactile robotic systems operating in the real-world for extended periods of time. In this work the sensory maps have been purposely distorted in order to evaluate the performance of the algorithm.

I. INTRODUCTION

The sense of touch will enable mobile autonomous platforms to explore, navigate and interact safely and robustly in unknown, unstructured environments. Sub-dermal (skin covered) and extra-dermal (whisker) tactile sensing are the two main paradigms of how the sense of touch has evolved in nature. Each are based on similar cutaneous structures and mechanoreceptors embedded in the skin, however, whiskers also comprise of a passive, flexible rod (hair) that protrudes out of the derma. Emulating the sensory capacity of touch in robotics is highly challenging with technological and physical issues being the major constraints. In the past decade, thanks to material science, progressive miniaturisation of electronics and technical advancements, the attention for this sense has thrived and a growing community is actively investigating different approaches to solve a wide range of issues related to touch. These include object recognition [1], navigation [2], and neuro-physiological model validation [3].

Whiskers are relatively robust to damage, they have no sensors along their length and deflections are processed by sensors at the base, which extends their perceptual range and protects the delicate sensory apparatus at the base from damage. These characteristics make whisker-like sensors an attractive solution for exploring environments where other sensory modalities such as vision and audition cannot be relied upon (e.g. in confined and visually occluded environments). Whiskers are mechanically simple and inexpensive elements that are fundamentally expendable as well as being relatively compliant and low-weight. A

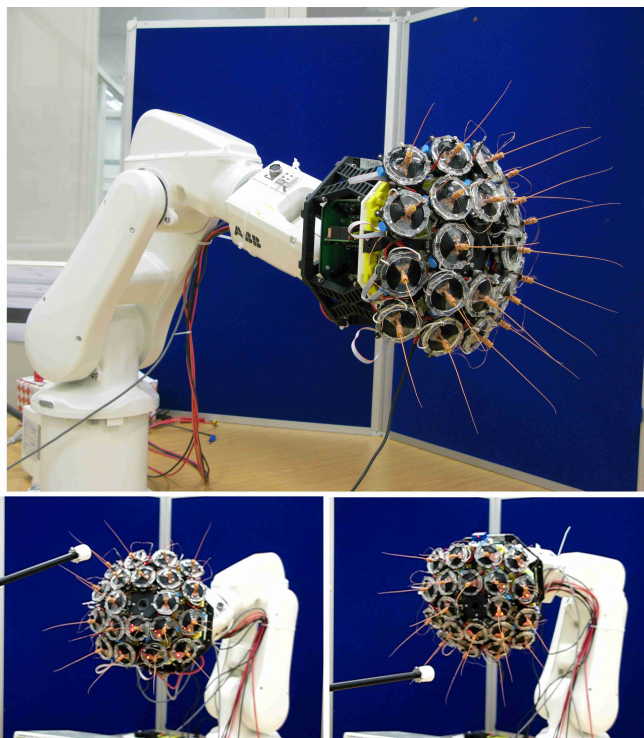


Fig. 1. **The BellaBot platform** consists of an array of 20x DEAP actuated tactile whiskers mounted onto a small 5 DoF industrial manipulator. The location of contacts made by the whiskers as they move through the environment are represented internally using a head centric map of space. This map is used to plan the motion of the robot such that the camera mounted at the centre of the whisker array is directed toward the point of contact as shown in the 2 lower video frames.

damaged whisker can simply be replaced (or ‘regrown’ in the natural case) cheaply and quickly. These features make whisker like sensors ideal for developing robots with tactile, touch sensors both in terms of maintenance costs and intrinsic safety in both human-robot and robot-environment interactions.

In recent years, a growing number of studies have focused upon different aspects of tactile sensing using whiskers from the mechanical [4], control [5] and capability [6] perspectives. Many bioinspired whiskered robots have also been developed to support these studies (see [4] for review). In this work we investigate adaptive sensorimotor learning using our current whiskered robotic platform “*BellaBot*” which has an array of 20 whisker-like tactile sensors, actuated using Di-electric Electro-Active Polymer (DEAP) technology, and attached to a 5 degrees-of-freedom industrial

¹Bristol Robotics Laboratory, University of Bristol and University of the West of England, Bristol, UK. tareq.assaf@brl.ac.uk

²Sheffield Robotics, University of Sheffield, Sheffield, UK

robotic arm (see figure 1). Here, we focus on the calibration of a head centred topographic map of whisker sensory space to improve the accuracy of directed motor commands toward points of interest in the map. Such a calibration is needed to adapt the sensorimotor map that represents the whisker array to variations caused by damaged or substituted whiskers over time. A bio-inspired adaptive control scheme, based on the adaptive filter model of the cerebellum [7], is used for map calibration in real-time robot experiments.

The following section describes the key components of the platform used in this study and an overview of how the adaptive filter algorithm has been applied to sensory map calibration. The methods section describe the experimental set-up, movement strategy of the robot and the modes of learning used to generate the results illustrated in the following section. The paper concludes with a discussion of the results and highlights directions for future work.

II. BACKGROUND

A. Platform

The robot platform *Bellabot* was developed as part of the Bella project (full name: Bioinspired Control of Electro-Active Polymers for Next Generation Soft Robots, funded by EPSRC grant number EP/I032533/1). It consists of a custom built structure, or *head*, that holds an array of 20 whisker-like tactile sensors mounted into individual DEAP based assemblies (see figure 2). The whiskers were 3D printed using an EnvisionTec machine from their proprietary photocure material called nanocure-25. The whiskers were 110 mm long, with a circular cross-section 1.3 mm diameter at the base tapering linearly to 0.3 mm at the tip. A small Neodymium magnet is fixed at the base of each whisker which, in turn, is held in an artificial follicle assembly by a polyurethane plug that acts as a universal joint and return spring. When at rest the magnet at the base of the whisker is positioned directly above a tri-axis Hall effect sensor IC (Melexis MLX333). As the magnet is displaced by deflections of the whisker shaft, the Hall effect IC generates 2 signals proportional to the magnitude of displacement in 2 orthogonal axes. These signals are sampled at 500Hz and passed via USB to the main control computer mounted externally to the *Bellabot* platform. Motor commands to move each whisker are subsequently relayed from the main control computer and converted to the high voltages ($\sim 4\text{KV}$) required to energise the DEAP actuators, described more fully in [8]. The DEAP actuators enable the whiskers to actively rotate at their base through $\pm 20^\circ$, generating motion analogous to the rhythmic whisking behaviour observed in small mammals such as rat [5]. This method of whisker actuation was incorporated into the platform as part of a broader exploration of cerebellar inspired adaptive control applied to non-linear, time varying plant [9], [10]. The head is attached as the end-effector to an industrial manipulator (ABB - IRB120), hereafter referred to as the *neck*. In this study, as explained in the introduction, we focus on utilising an adaptive filter algorithm to calibrate a whisker sensory

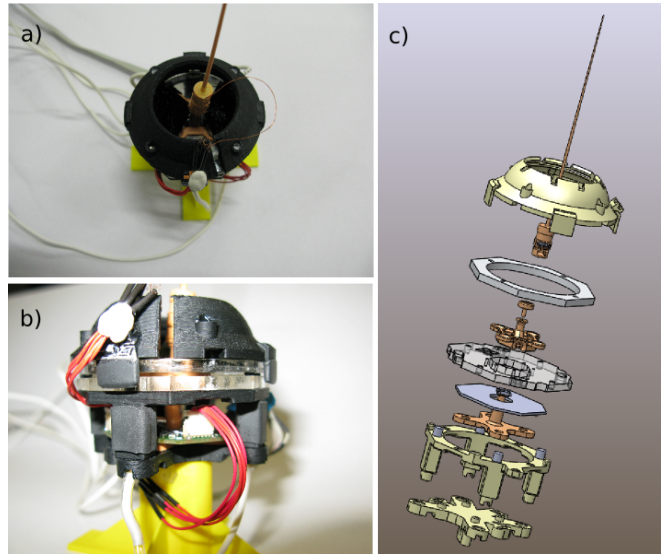


Fig. 2. An individual DEAP actuated whisker module. **a)** view from above highlighting EAP membrane **b)** view of electronics and assembly from side. **c)** Exploded CAD rendering of the overall assembly without the EAP membrane.

map representing the head space of *Bellabot*. To enable this we have modelled the *orienting* behaviour observed in whiskered mammals, whereby the animal will rapidly direct its tactile fovea (typically snout) toward points of unexpected whisker contact [11]. In the mammalian brain this ability is orchestrated by a structure called the superior colliculus that uses a head centric map of multi-modal sensory space to initiate motor primitives to rapidly attend to prey or avert from predators [12]. The *Bellabot* implementation of this behaviour uses a map of the surface of the volume occupied by the tactile whisker array, i.e., the plane represented by interpolating between the whisker tips. As the whiskers are *whisked* (driven by the DEAP actuators at their base) their angle of rotation is monitored using miniature Hall effect shaft encoders. In addition, the odometry from the neck is also monitored allowing a simple geometric transform to be applied between the individual whisker sensor frames and the global frame required for directing the neck and head toward points of whisker contact, i.e., orienting. The same approach to directing the exploratory attention of a whiskered robot has been demonstrated before [13], however, here we directly address how the accuracy of such orients can be improved. The problem partly lies in the assumptions made in constructing the geometric transforms; firstly, all contacts are assumed to occur at the tip of the whisker; secondly, the whiskers are assumed to be rigid beams of known length; and thirdly, the whisker tips are assumed to be coaxially aligned with the whisker base. In reality each of these assumptions can fail due to poor manufacturing tolerances, accumulated damage, droop caused by gravity, bending of the whisker shaft during contact, and so on. To accommodate these inaccuracies we propose to iteratively calibrate the sensory map such that successive orients become more accurate irrespective of the originally fixed geometric assumptions

made in the transformation between frames. The details of the algorithm used are presented in the following sub-section, suffice to say here that a measure of error from each orient is required to train the algorithm. This was derived from images taken by a standard USB camera mounted at the centre of the whisker array (see figure 1). Upon completion of the orient by the robot toward the estimated point of contact an image was captured of the the known contact object, a small ball fixed to the end of a rod as shown in figure 1 and in the supplementary video. The difference in desired position (centre of image) to actual position of the ball was then passed to the calibration algorithm as the error.

B. Adaptive filter model of map calibration

As mentioned in the introduction, a bio-inspired adaptive control scheme based on the adaptive filter model of the cerebellum [14], [15], [7] was used to calibrate a 2D topographic map [16] of the whisker sensory space.

During active whisking the whisker rotation and vibration sensory streams were continuously recorded [8]. Vibration signals were thresholded to remove the noise generated by self-motion (or *re-afferent noise*) by setting signals below threshold to zero. Detected targets (i.e. when vibration signals on individual whiskers were above threshold for a number of samples) were then written into the topographic map using a 2D Gaussian to provide a probabilistic representation of the target location (Fig. 3a). The Gaussian centre was placed at the assumed tip of the contacted whisker, with the centre of the head defined as the origin of the map. Errors in the target (ball) position were only provided in two dimensions (in-plane with the camera), therefore, the estimated perpendicular distance to a detected target was fixed.

The cerebellar algorithm was used to shift the topographic map of the estimated target location to improve the accuracy of subsequent orients. This was done by implementing a global bias in the x - and y - directions. For a given sensory map with a target center at estimated location $\mathbf{x} = (x, y)$, the cerebellar bias input $\mathbf{z} = (\delta x, \delta y)$ will make it look as though the target has center $\mathbf{x} + \mathbf{z}$. In effect the cerebellum ‘slides’ the map activity across the map by an amount $\mathbf{z} = (\delta x, \delta y)$.

The cerebellar bias was calculated as a sum of the weighted (Fig. 3c) *parallel fibre signals*. The parallel fibre signals, \mathbf{p} in the cerebellar algorithm [15], [7], were assumed to carry normalised, coarse coded versions of the topographic map (Fig. 3b), i.e., the map representing the sensory space was decomposed into a regularly distributed array of 64 (8x8) nodes (each representing a parallel fibre) with the total cerebellar bias calculated as:

$$\delta x = \sum \mathbf{w}_x \mathbf{p} \quad (1)$$

$$\delta y = \sum \mathbf{w}_y \mathbf{p} \quad (2)$$

The weights w_x and w_y of each parallel fibre are learnt over trials (from initially zero) using the covariance learning rule [17]. Here we assume the *climbing fibre* teaching signal inputs to the adaptive filter model carry signals related to the

x , y components of target acquisition error so the learning rule for estimating these weights can be written as

$$\Delta \mathbf{w}_x = -\beta e_x \mathbf{p}' \quad (3)$$

$$\Delta \mathbf{w}_y = -\beta e_y \mathbf{p}' \quad (4)$$

where β is the learning rate, and e_x, e_y the target errors acquisition in the x and y directions respectively.

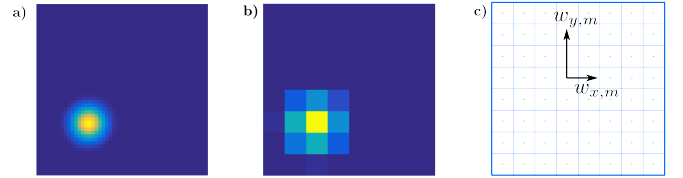


Fig. 3. Interface between map of head space and the adaptive filter. a) A positive whisker contact generates a Gaussian activity in the topographic map centred at the estimated point of contact. b) The map is coarse coded into discrete 2D cells. c) Each cell has an associated weight vector x, y , represented by the m^{th} parallel fibre entering the adaptive filter. Each weight vector is proportionally modified by the filter in response to orient errors to calibrate the overall map.

III. METHOD

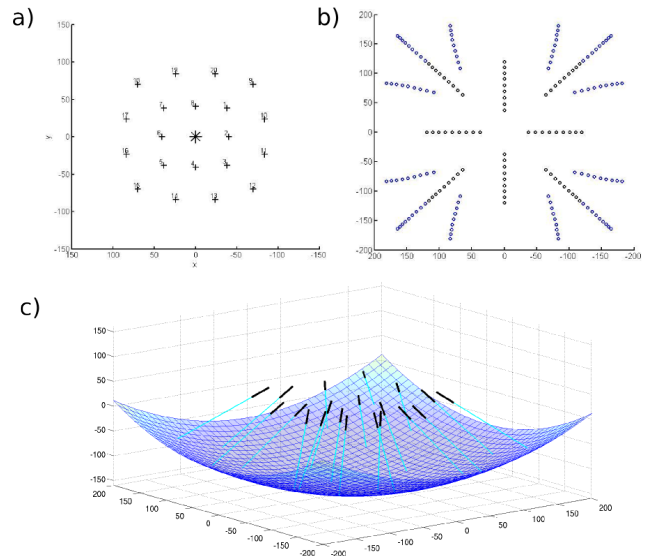


Fig. 4. Maps of whisker sensory space in head centric frame. a) 2D projection of base locations of whiskers 1-8 occupying the inner circle, and 9-20 the outer circle. The asterisk at the origin indicates the location of the camera. b) 2D representation of the arcs generated by each whisker tip during whisking, each point indicating 5° of travel. c) 3D projection of the surface created through interpolation of whisker tip locations.

To generate training data and to evaluate the performance of the adaptive filter, the contact ball was mounted onto a portable adjustable clamp stand and positioned in front of the Bellabot platform. The Bellabot was programmed to cyclically perform 4 sequential behaviours:

- **Explore:** The whisker array would whisk at a fixed rate whilst the neck moved the head forwards until a contact was made by one of the whiskers.

- **Recoil:** The whiskers would stop whisking and the neck would move the head backwards a short distance for safety.
- **Orient:** The head would be moved such that the centre mounted camera is directed toward the estimated point in space as determined by the head-centric topographic map of whisker sensory space. At the end of the orient an image is captured from the camera.
- **Reset:** the Bellabot would return to its original start configuration before switching back to the Explore behaviour.

Between behavioural cycles the contact ball was either left in position such that the same whisker would be touched again or was relocated to touch another. In both cases the ball was positioned such that no more and no less than 1 whisker would make contact in each explore phase of the cycle. The supplemental video associated with this paper shows an example of the cyclical behaviour of Bellabot during a typical experiment. It begins part way through a recoil and orient following which the contact ball is relocated, the Bellabot then resets before repeating the cycle. The images taken at the end of each orient phase were processed to extract an error vector which, in turn, was used to train the adaptive filter and thereby modify the map. To evaluate the performance of the system a set of trials were conducted using known errors in the map, i.e., the true geometric mappings between the whisker tips and world frame, as shown in figure 4, were purposefully misaligned or *morphed*. These morphed maps were classed into 4 different types as described below and summarised for reference in figure 5. Note that for clarity, only the whisker tip locations of the 8 whiskers that occupy the inner circle of the array are shown.

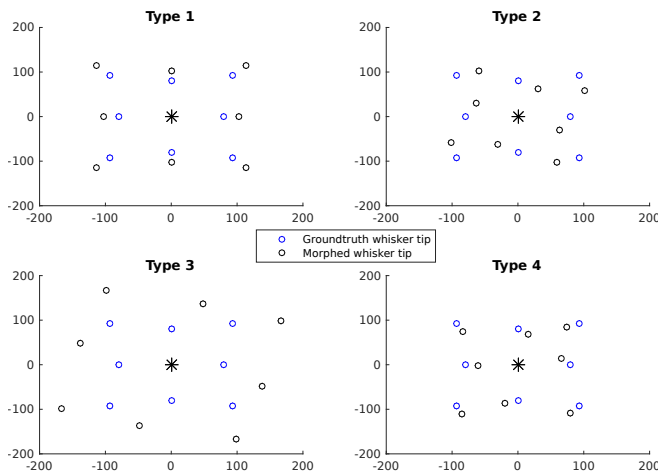


Fig. 5. 2D representation of whisker tip locations in head-centric space for each of the morphed maps used to test the adaptive filter algorithm. Type 1) uniform expansion; Type 2) uniform rotation; Type 3) uniform expansion and rotation; Type 4) random rotation with uniform translation

- **Type 1)** The magnitude of the polar coordinates of the true whisker base locations were increased by $\sim 30\text{mm}$, i.e., uniform expansion.
- **Type 2)** The angle of the polar coordinates of the true

whisker base locations were increased $+\pi/4$ radians (clockwise direction), i.e., uniform rotation

- **Type 3)** The whisker base coordinates were both uniformly expanded and rotated as above.
- **Type 4)** Each whisker base was translated by 20mm in a random direction ($\pm\pi$ radians) centred on the ground truth of that whisker.

IV. RESULTS

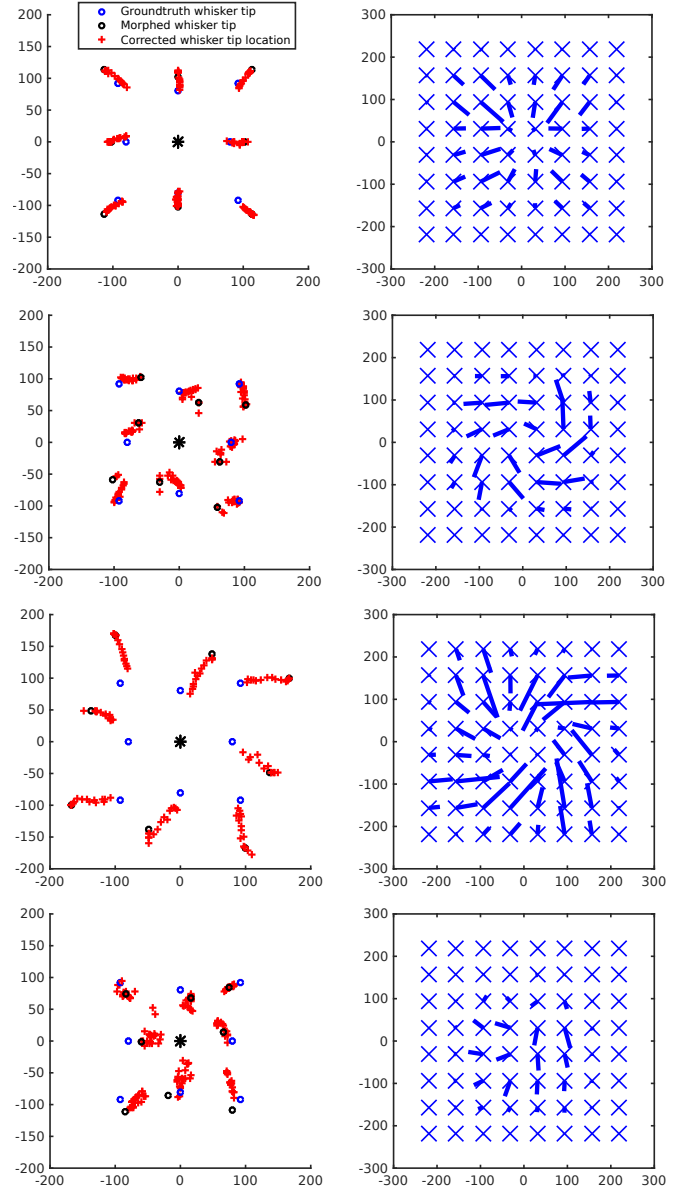


Fig. 6. Summary of corrections made to the estimates of whisker tip locations by the adaptive filter applied to the 4 morphed map types. Each row represents a morphed map type (1-4), the left panels show the evolution of whisker tip estimates in head space from original morphed location toward ground truth following each whisker contact event. The right panels summarise the final trained weight vectors associated with each of the 64 parallel fibres that represent the whisker sensory space.

The training data for the adaptive filter was gathered by repeatedly performing the behavioural cycles described in the methods section using two different protocols. The

first was referred to as *tapping*, whereby the contact ball remained in position between cycles for a fixed number of iterations (typically 15). The second involved *randomly*

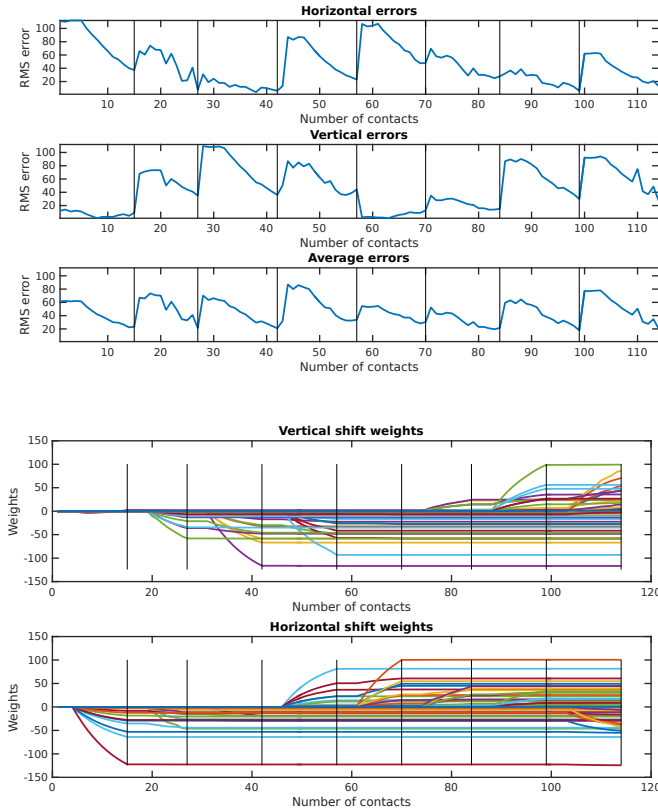


Fig. 7. **Top)** Averaged RMS errors between the original morphed map (Type 3) and the actual map as determined through visual feedback following orients toward contact with the ball by the whisker array. The vertical bars indicate when the ball was relocated between behavioural cycles to make contact with another whisker. **Bottom)** Evolution of the weight vectors associated with each of the 64 parallel fibres that constitute the adaptive filter model of the cerebellar algorithm during the same experiment as shown in the error plots above.

relocating the contact ball such that it will be touched by a different whisker in subsequent cycles. The results shown in figure 6 summarise the corrections made by the filter to the estimate of whisker tip locations following repeated contact with the whisker array for all 4 morphed map types using the tapping protocol. In all cases the algorithm was successful in reducing the errors introduced into the map, irrespective of the tapping or random protocol adopted. This is illustrated in the figure by the trend of the whisker tip estimates (red crosses) moving from the morphed whisker tip locations toward their ground truth locations. Accordingly, the change in the weight vector space of the adaptive filter reflects this adaptation, effectively distorting the original erroneous map into a better representation of the real-world. Figure 7 shows how the weight vectors (x - horizontal, y - vertical) of the filter elements, representing the parallel fibres, change as the whiskers made contact with the ball. This data was captured during the tapping experiments using morphed map type 3 (expanded and rotated), with the vertical bars indicating when the ball was relocated to touch a

new whisker. Using this training protocol resulted in an irregular error distribution whereby each region of the map surrounding the whisker currently tapping the ball would be modified in isolation. Using the training protocol where the ball was randomly relocated between subsequent behavioural cycles such that different whiskers would make contact, as shown in figure 8, produced a more consistent error reduction across the map which better demonstrates the generality of the learning algorithm.

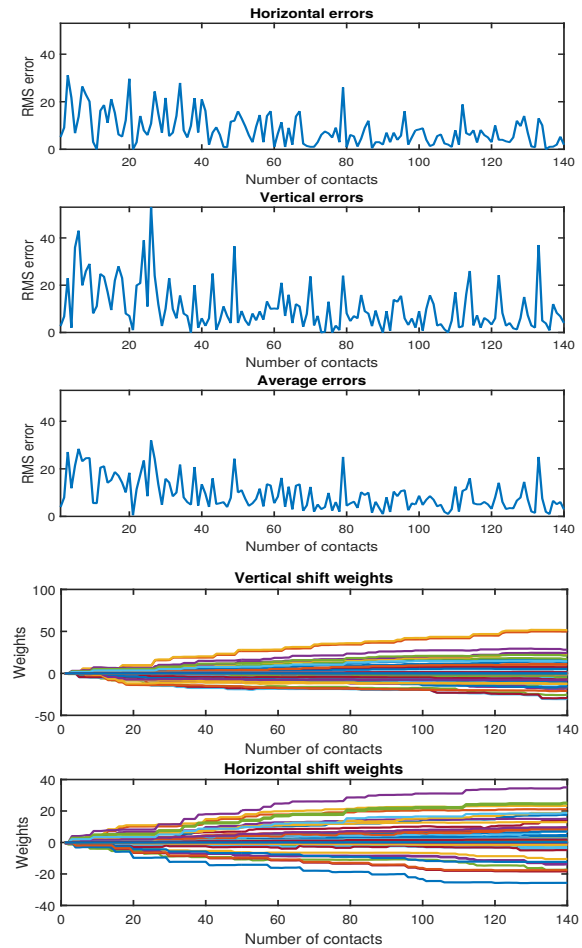


Fig. 8. RMS error plots and weight space evolution as described in figure 7 during the random training protocol on morphed map type 1. The ball is re-located between each behavioural cycle (indicated here as individual contacts) to touch a different whisker leading to a more generalised training of the map

V. DISCUSSION

An adaptive filter model of cerebellar function has been applied to sensory map calibration and demonstrated as a plausible candidate for further investigation. The results show that even with a relatively coarse encoding of the sensory space, here represented using just 64 parallel fibres, the algorithm is capable of significantly reducing the error introduced from a variety of distorted map morphologies. Of these morphed maps the algorithm performed less well when presented with the random rotation type (type 4) as

opposed to the uniform distortions of type 1-3 which is concordant with prior expectations. However, the evident reduction in map error for type 4 was greater than expected considering the resolution afforded by the limited number of parallel fibres in the filter. The experiments also revealed what was at first interpreted as a systematic error for whisker number 8, whereby, following training the learnt tip location was consistently offset from its assumed ground truth. On closer inspection it was found that the algorithm was actually correcting for an intrinsic bend in this whisker as shown in figure 9. The filter was, therefore, correcting for the false assumption that the tip of the whiskers were co-axially aligned with their bases which provides an intriguing insight into the potential of this approach.

The principle direction for improvement in future work

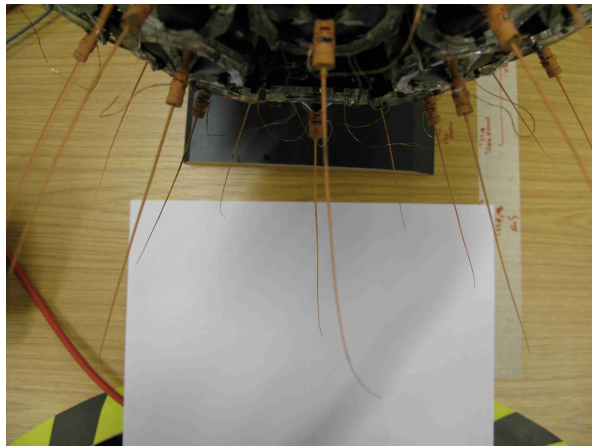


Fig. 9. Photograph taken from directly above the head of Bellabot highlighting the intrinsic bend in whisker number 8 that was accommodated into the calibrated map

stems from the observation that the reduction in error for the estimates of whisker tip locations of whiskers in the outer circle (9-20) were marginally less than the inner circle (1-8). This has been interpreted as the effective non-linearity introduced by the 2D projection of the 3D whisker tip surface being more pronounced for the more distally located whiskers in the outer circle of the array (see figure 4c). This could be accommodated by introducing a non-linearity into the algorithm, either by replacing the currently linear parallel fibre elements with a non-linear operator, or through a non-uniform parallel fibre representation of the sensory space. In conclusion, perhaps the most exciting outcome from this preliminary investigation has been that through only a small extension of an existing model of cerebellar functionality originally applied to motor learning, we have demonstrated that it is also well disposed to the task of sensory map calibration.

ACKNOWLEDGMENT

This work was funded by the EPSRC through grant reference number EP/I032533/1

REFERENCES

- [1] A. Aggarwal and F. Kirchner, "Object recognition and localization: The role of tactile sensors," *Sensors*, vol. 14, no. 2, p. 3227, 2014. [Online]. Available: <http://www.mdpi.com/1424-8220/14/2/3227>
- [2] M. J. Pearson, C. Fox, J. C. Sullivan, T. J. Prescott, T. Pipe, and B. Mitchinson, "Simultaneous localisation and mapping on a multi-degree of freedom biomimetic whiskered robot," in *Robotics and Automation (ICRA), 2013 IEEE International Conference on*. IEEE, 2013, pp. 586–592.
- [3] S. R. Anderson, J. Porrill, M. J. Pearson, A. G. Pipe, T. J. Prescott, and P. Dean, "An internal model architecture for novelty detection: Implications for cerebellar and collicular roles in sensory processing," *PLoS ONE*, vol. 7, no. 9, 09 2012.
- [4] T. Prescott, M. Pearson, B. Mitchinson, and T. Pipe, "Whisking with robots: From rat vibrissae to biomimetic technology for active touch," *IEEE Robotics and Automation Magazine*, vol. 16, pp. 42–50, 2009.
- [5] R. W. Berg and D. Kleinfeld, "Rhythmic whisking by rat: Retraction as well as protraction of the vibrissae is under active muscular control." *J Neurophysiol*, vol. 89, no. 1, pp. 104–117, Jan 2003.
- [6] G. Carvell and D. Simons, "Biometric analyses of vibrissal tactile discrimination in the rat," *The Journal of Neuroscience*, vol. 10, no. 8, pp. 2638–2648, 1990.
- [7] P. Dean and J. Porrill, "Evaluating the adaptive-filter model of the cerebellum," *The Journal of physiology*, vol. 589, no. 14, pp. 3459–3470, 2011.
- [8] M. J. Pearson and T. Assaf, "High speed switched, multi-channel drive for high voltage dielectric actuation of a biomimetic sensory array," in *Biomimetic and Biohybrid Systems*, ser. Lecture Notes in Computer Science. Springer International Publishing, 2014, no. 8608, pp. 414–416.
- [9] E. D. Wilson, T. Assaf, M. J. Pearson, J. M. Rossiter, P. Dean, S. R. Anderson, and J. Porrill, "Biohybrid control of general linear systems using the adaptive filter model of cerebellum," *Frontiers in Neurobotics*, vol. 9, no. 5, 2015. [Online]. Available: <http://www.frontiersin.org/neurobotics/10.3389/fnbot.2015.00005>
- [10] T. Assaf, J. Rossiter, and M. Pearson, "Contact sensing in a bio-inspired whisker driven by electroactive polymer artificial muscles," in *Sensors, 2013 IEEE*, Nov 2013, pp. 1–4.
- [11] R. A. Grant, A. L. Sperber, and T. J. Prescott, "The role of orienting in vibrissal touch sensing," *Frontiers in Behavioral Neuroscience*, vol. 6, no. 39, 2012. [Online]. Available: <http://doi.org/10.3389/fnbeh.2012.00039>
- [12] P. Dean, P. Redgrave, and G. Westby, "Event or emergency? two response systems in the mammalian superior colliculus," *Trends in neuroscience*, vol. 12, no. 4, pp. 137–147, 1989.
- [13] B. Mitchinson, M. J. Pearson, A. G. Pipe, and T. J. Prescott, "Biomimetic tactile target acquisition, tracking and capture," *Robotics and Autonomous Systems*, vol. 62, no. 3, pp. 366 – 375, 2014.
- [14] M. Fujita, "Adaptive filter model of the cerebellum," *Biological cybernetics*, vol. 45, no. 3, pp. 195–206, 1982.
- [15] P. Dean, J. Porrill, C.-F. Ekerot, and H. Jörntell, "The cerebellar microcircuit as an adaptive filter: experimental and computational evidence," *Nature Reviews Neuroscience*, vol. 11, no. 1, pp. 30–43, 2010.
- [16] E. Wilson, P. Dean, S. Anderson, and J. Porrill, "Cerebellar calibration of topographic maps in the superior colliculus using the adaptive filter model," vol. 23, no. P3-C-014. British Neurosci. Assoc. Abstr., 2015.
- [17] B. Widrow and S. D. Stearns, "Adaptive signal processing," *Englewood Cliffs, NJ, Prentice-Hall, Inc.*, vol. 1, 1985.